

High-Throughput Reaction Optimisation and Activity Screening of Ferrocene-Based Lewis Acid–Catalyst Complexes by Using Continuous-Flow Reaction Detection Mass Spectrometry

Cornelius T. Martha,^{*,[a]} Anton Heemskerk,^[a] Jan-Carel Hoogendoorn,^[a] Niels Elders,^[b] Wilfried M. A. Niessen,^[a] Romano V. A. Orru,^[b] and Hubertus Irth^{*,[a]}

Abstract: Optimising synthetic conversions and assessing catalyst performance is a tedious and laborious endeavour. Herein, we present an automated alternative to the commonly applied sequential approaches that are used to increase catalyst discovery process efficiencies by increasing the number of entities that can be tested. This new approach combines conversion of the reactants and determination of product formation into a single comprehensive reaction detection system that can be operated with minimal catalyst and reactant consumption. With this approach, rudimentary reaction

conditions can be quickly optimised and the same system can then be used to screen for the optimal homogenous catalyst in a selected solution-phase synthetic conversion. The system, which is composed of standard HPLC components, can be used to screen catalyst libraries at a repetition rate of five minutes and can be run unsupervised. The sensitive mass spectrometric

detection that is implemented in the reaction detection methodology can be used for the simultaneous monitoring of reactants, catalysts and product ions. In the experiments, the three-component reaction that gives a substituted 2-imidazoline was optimised. Afterwards, the same method was used to assess a library of ferrocene-based Lewis acid catalysts for performance in the aforementioned conversion in six different solvents. We demonstrate the feasibility of using this methodology to directly compare the performance results obtained in different solvents by calibrating the solvent-specific MS responses.

Keywords: high-throughput screening • homogeneous catalysis • mass spectrometry • multicomponent reactions • reaction optimization

Introduction

Innovation in chemical industrial processes is a perpetual process driven by an incessant need to reduce the consumption of resources and energy and the production of waste in an everlasting attempt to be more competitive by reducing

costs. Nowadays, industrial progress includes the need to develop sustainable processes in which environmental impact is not amplified when economic growth is achieved. Of all the approaches that are used to decrease the environmental footprint, catalysis is one of the most important tools due to its principal role in industrial chemical synthesis.

With industry demands to lower development costs, catalyst discovery process efficiencies have to be increased. A possible strategy is to replace conventional sequential synthesis and activity assessment methods by automated high-throughput experimental methodologies. This combinatorial approach requires the development of specific instruments and robotics to cope with the demanded throughput that originates from the large number of samples.^[1] Spectroscopy-based techniques for the detection of catalytic activity in high-throughput screening assays are still the most ubiquitous methods in this field despite the restricted applicability caused by the prerequisite of chromophores and fluorophores in either substrate or product for detection.^[2] In this perspective, mass spectrometry (MS) offers an outstandingly

[a] C. T. Martha, A. Heemskerk, J.-C. Hoogendoorn, Prof. Dr. W. M. A. Niessen, Prof. Dr. H. Irth
Department of Analytical Chemistry and Applied Spectroscopy
Faculty of Sciences, VU University Amsterdam
De Boelelaan 1083, 1081 HV Amsterdam (The Netherlands)
Fax: (+31) 205987542
E-mail: ctmartha@few.vu.nl
irth@few.vu.nl

[b] N. Elders, Prof. Dr. R. V. A. Orru
Department of Organic and Inorganic Chemistry
Faculty of Sciences, VU University Amsterdam
De Boelelaan 1083, 1081 HV Amsterdam (The Netherlands)

Supporting information for this article is available on the WWW under <http://dx.doi.org/10.1002/chem.200900317>.

wide range of applicability for the sensitive detection of (multiple) selected target analytes in complex samples.^[3] Although quantification can be affected by ion suppression and there are compounds that are not ionisable, the multitude of gas- and solution-phase mechanisms that convert neutral molecules into ionic species (i.e., protonation, metalation, chemical reactions, quaternisation and oxidation/reduction) results in the eminent potential of MS for the identification of catalyst complexes.^[4]

Although several combinatorial tools have been developed for the catalysis toolbox, their development into high-throughput reaction optimisation strategies is relatively untapped despite the fact that attractive new analytical platforms have been introduced.^[5] For reaction optimisation in material research, research efforts are mainly focused on the development of new *in silico* design, improved reactor platforms and analysis tools.

Commonly, the optimisation of reaction parameters is performed by sequential unit operations, such as transfer of liquids, quenching of the reaction and storage of the samples prior to analysis. In the most advanced unit-operation-based methodologies, automated workstations and robotics are used to complete the sequential steps.^[6]

Recently, a continuous-flow reaction detection screening system was introduced that was used for the determination of catalyst performance in synthetic conversions.^[7] The feasibility of using this approach for the assessment of catalyst activity towards a selected synthetic conversion was demonstrated by the performance screening of a selected number of homogeneous Lewis acid catalysts for a synthetic conversion in tetrahydrofuran (THF). The results proved to be comparable to the results obtained with a traditional bench-scale experiment. Moreover, the mass spectrometric detection proved to be very sensitive, with an achieved detection limit of as low as 1.6 nM for the formed product, while the ruggedness of the method was illustrated with a 24-hour screening that was completed with a peak-area variation of within 7% relative standard deviation.

Herein, the applicability of the novel continuous-flow reaction detection methodology is explored. Initially, the feasibility of using this reaction detection methodology for the high-throughput reaction optimisation of a Lewis acid-catalysed multicomponent synthesis of substituted 2*H*-2-imidazolines was investigated. Secondly, by utilising the same comprehensive system, the catalyst–ligand activity of different ferrocene-based catalyst complexes in this atom-efficient multicomponent reaction (MCR) in six different commonly used solvents was assessed.

Results and Discussion

In general, the workflow of a catalysed reaction optimisation strategy includes 1) the selection of the synthetic conversion, 2) a preliminary selection of potential catalysts, 3) the optimisation of the synthetic conversion of reactants by selected variation of involved system parameters and

4) the determination of product formation at associated parameter settings to optimise product formation. Once the optimal settings have been determined, a catalyst performance screening can be used to identify the best-performing catalyst for the selected synthetic conversion.

In commonly applied catalyst performance screening methods, catalyst performance is rated based on kinetics that are constructed from the increased slope of the initial rate of the reaction. To obtain this data in traditionally applied methodologies, the conversion of reactants into products has to be determined at different reaction times. In the continuous-flow reaction detection methodology, an increased throughput is accomplished by a reduction in the number of data points that are obtained. In the reaction detection approach, the conversion into product takes place in a thermostated reactor with a fixed internal volume. Therefore, the catalyst performance is assessed by determining the peak area from the selected ion monitoring (SIM) product trace in atmospheric-pressure chemical ionisation (APCI) MS detection. The optimal continuous-flow reactor volume in this system associates with a reaction time that only slightly exceeds the time period required for the reaction to reach its initial rate. For this methodology to be applicable, it should allow for the sensitive quantification of the product with high accuracy. In the current continuous-flow reaction detection setup, this is accomplished with system parameters, that is, sampling time, reaction time, reaction pressure and reaction temperature, that are either fixed or accurately controlled and result in high system repeatability and reproducibility.

The optimisation of a certain reaction is usually performed by relating product formation to different reaction parameter settings. Herein, we present an integrated analytical reaction detection methodology based on standard HPLC equipment (see Figure 1). An advantage of this continuous-flow total-analysis system is that all the intermediate liquid transfer steps are made superfluous and the necessity of applying robotics to achieve a high sample throughput is circumvented. In a sequential unit operation system, product formation is determined at different reaction settings. We

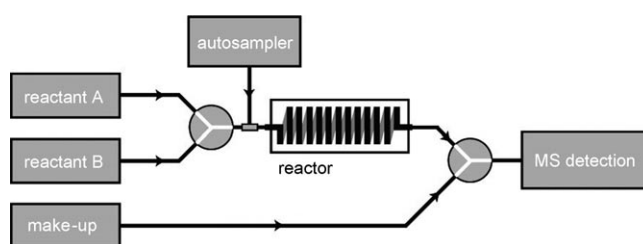
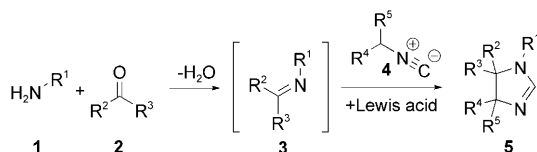


Figure 1. Schematic overview of the continuous-flow reaction detection system. This system is comprised of two HPLC pumps labelled reactant A and reactant B, which pump the reactants (**3** and **4**, respectively, see Scheme 1) into a mixer. An injector is used to introduce the catalysts into the stream of reactants. The conversion of reactants into product takes place in the thermostated coiled open tubular reactor. A third HPLC pump (make-up) can be used to add water to quench the reaction and increase APCI-MS detection compatibility.

demonstrate that accurately controlled system parameters can be used for the optimisation of reaction parameters.

After reaction optimisation, the flexibility of the system was demonstrated by employing the same mass spectrometric detection system for the screening of catalyst libraries for activity towards a selected synthesis. Minute amounts of reactants and catalysts were used, without the necessity of altering any system parameters.

Lewis acid catalyst selection: Lewis acids have been reported to be excellent catalysts in the MCR of a substituted 2*H*-2-imidazoline of type **5** (Scheme 1).^[8] In this MCR, an



Scheme 1. Lewis acid-catalysed three-component reaction giving 2*H*-2-imidazoline (R^1 = Benzyl, $R^2 = R^3 = \text{CH}_3$, $R^4 = p$ -nitrobenzyl, $R^5 = \text{H}$).

amine (**1**) condenses with a ketone or aldehyde (**2**) to form an intermediate imine (**3**) that subsequently reacts with an α -acidic isocyanide (**4**). This atom-efficient reaction, with water as the only byproduct, is ideally suited for the generation of focused libraries of pharmaceutically interesting analogues by using a combinatorial approach in which molecular diversity is rapidly introduced by varying the substituents of the reactants.^[9] Additionally, sample pre-cleanup costs are significantly reduced due to the atom efficiency. New 2-imidazolines are promising pharmaceutical candidates.^[10] For example, their affinity towards the imidazoline binding site result in a broad range of pharmaceutical applications with a wide variety of associated biological functions, such as hypertension, blood pressure regulation, insulin secretion control and numerous human brain disorders.^[11] Moreover, 2-imidazolines are used as chiral templates to increase reaction enantioselectivity in asymmetric synthesis.^[12]

The experiments herein describe the conversion of benzylamine (**1**; R^1 = benzyl) and acetone (**2**; $R^2 = R^3 = \text{CH}_3$) into the corresponding intermediate imine (**3**) followed by a Lewis acid-catalysed reaction with *p*-nitrobenzylisocyanide (**4**) to form the corresponding 2*H*-2-imidazoline (**5**).

In the first step of the reaction optimisation experiments, eight triflates ($\text{Zn}(\text{OTf})_2$, $\text{Yb}(\text{OTf})_3$, LiOTf , $\text{Hf}(\text{OTf})_4$, AgOTf , $\text{Sc}(\text{OTf})_3$, $\text{Cu}(\text{OTf})_2$ and $\text{Bi}(\text{OTf})_3$) were screened for activity towards the synthesis of **5**. In this screening experiment, the triflates were injected at a repetition rate of five minutes. During the 40-minute experiment, 10 nmol ($\approx 4 \mu\text{g}$) of catalyst and 12 μmol ($\approx 2 \text{ mg}$) of reactants were consumed. As indicated in Figure 2, the best-performing triflate for this conversion is AgOTf . This Lewis acid catalyst was combined with a representative ferrocene (**6b**) to form the catalyst complex that was used for the further reaction optimisation experiments.

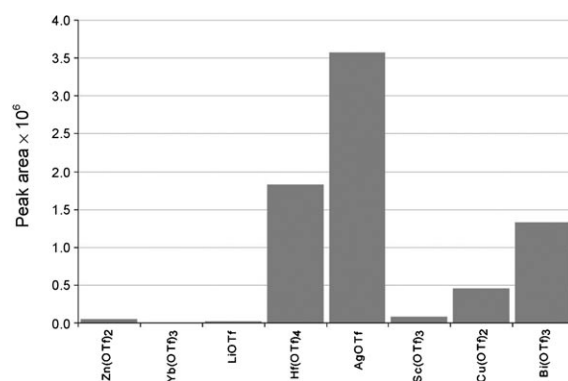


Figure 2. Integrated peak areas of the Lewis acid catalyst screening obtained with the continuous-flow reaction detection system, showing the activity of eight different metal-based triflates in the synthesis of **5**.

Reaction optimisation: In the reaction optimisation experiment described hereafter, the concentration of the reactants was fixed at 4 mM. The reactant ratio, catalyst concentration and reaction temperature were optimised by varying the associated system parameters in the analysis system. In Figure 3, the optimisation of the reactant ratio is presented.

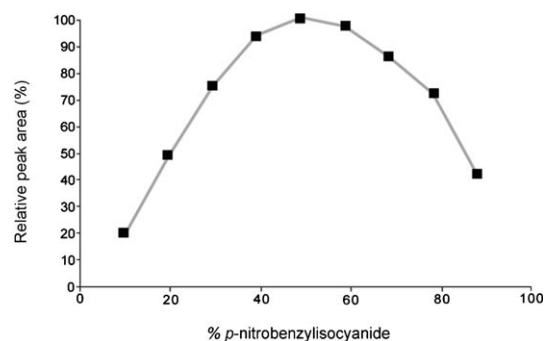


Figure 3. Relative peak areas of formed product determined by using MS detection at different substrate ratios. The normalised peak area illustrates the impact of reactant ratio on product formation.

In this experiment, the percentage of **4** was increased stepwise in increments of 10 % (nine steps).

The product formation was determined at different reactant ratios, whereas the conversion was catalysed by injecting 10 μL of the ligated AgOTf catalyst complex formed by mixing 1 mM AgOTf with an equal amount of ferrocene **6b** (Figure 4). With a repetition time of five minutes, this rapid optimisation strategy was performed by automatically changing the reactant A/reactant B ratio by altering the flow rate of the HPLC pumps, as depicted in Figure 1, while the total flow remained unchanged. The associated product formation was determined by integration of the peak in the recorded SIM trace of the protonated product molecule (m/z 310.2). As shown in Figure 3, the ratio of reactants in the MCR has a significant effect on the overall product formation that can be achieved. If the peak areas at different ratios are normalised, a ratio of 50:50 **3/4** results in the high-

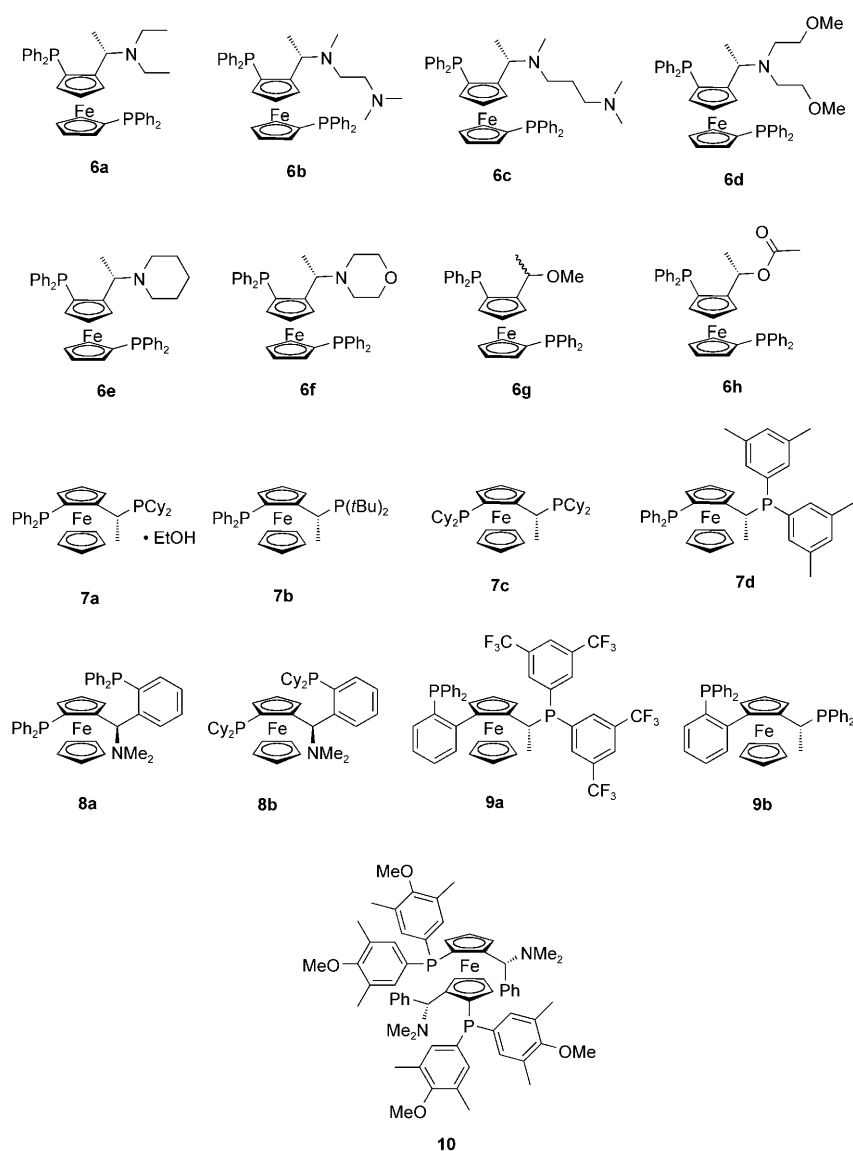


Figure 4. Stabilising ferrocene catalyst ligands. Ferrocenes **6a–h** share a common ferrocenic backbone with different substituents. Mixing the ferrocenes with AgOTf resulted in catalyst complexes that were screened for activity towards the synthesis of **5**.

est product yield. The ratio proved to be very important because a 20 % reduction in either of the reactants resulted in a 25 % decrease in product formation.

To optimise the catalyst concentration at the determined reactant concentration (4 mM), equal amounts of ferrocene **6b** and AgOTf were mixed and injected into the reaction detection system at different concentrations. The amount of product formed was determined by using the same methodology that was used in the previous experiment.

Figure 5 presents the product formation at twelve different catalyst concentrations between 500 nM and 500 μ M. Although the presence of the lowest catalyst concentration could be confirmed in the total-ion current (TIC) trace recorded by using a single quadrupole mass spectrometer, it did not result in enhanced product formation. At higher cat-

alyst concentrations the product formation increased significantly, with a maximum at the highest catalyst concentration. However, the product that formed did not increase linearly with catalyst concentration and an asymptotic curve was determined due to saturation of the reaction mixture. From the results of this experiment, the optimal catalyst–reactant ratio could be determined. At the lowest ferrocene-based catalyst concentration that showed activity, a catalyst/reactant ratio of 0.0125 % was applied. This ratio increases to 12.5 % (catalyst/reactant) at the highest catalyst concentration (500 μ M). From Figure 5, it can be concluded that increasing the catalyst concentration beyond 100 μ M (2.5 %) does not significantly improve the amount of product formed. Therefore, the optimum catalyst/reactant ratio is found to be 2.5 %.

Because the rate constant of a reaction is dependent on the reaction temperature, increasing the reactor temperature results in enhanced product formation. The temperature dependence of this MCR to give **5** has been investigated previously.^[7] By introducing the AgOTf catalyst at different temperatures, an optimum temperature curve was obtained. Although the highest temperature yielded

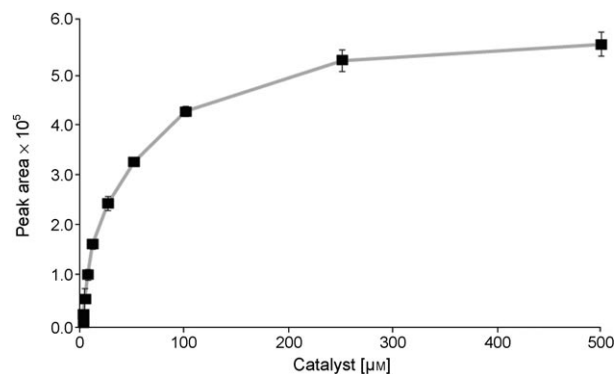


Figure 5. Peak areas of formed product determined at different catalyst concentrations during optimisation.

the highest product formation, the curve approached an optimum at 80°C. To determine the optimum temperature when stabilising ferrocene catalyst ligands are utilised, a mixture of 1 mM AgOTf and 1 mM ferrocene **6b** was injected at different reactor temperatures.

The results of the temperature optimisation experiment are presented in Figure 6. The data present an obvious in-

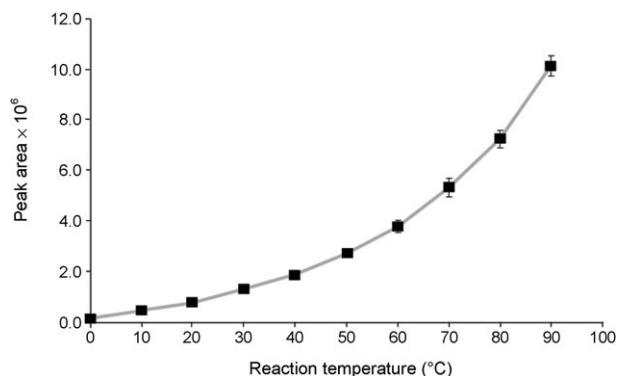


Figure 6. Reaction temperature optimisation.

crease in product formation (rate constant) at elevated temperatures. However, compared with previously obtained results the effect of enhanced reactor temperature is significantly larger. The differences are quite significant, especially when higher temperatures are applied. When recording the temperature curve, an optimum was not achieved because only reactor temperatures of up to 90°C were investigated. As the differences between the results of the temperature optimisation experiments with the two different catalyst classes suggest, temperature optima proved to be catalyst-class specific.

System development: One of the reasons for the popularity of spectroscopic detection techniques in the determination of catalyst performance is the versatile applicability of those methods. Although MS detection offers superior selectivity and sensitivity, and an ample number of applications for organometallic and inorganic compounds in solvents other than those commonly used in HPLC analysis are reported, the merits of this detection technique for synthetic conversions have not been fully explored yet. One of the important factors when considering the application potential in synthetic organic chemistry is the possibility of applying MS detection in virtually any desirable solvent. To demonstrate this ability, the catalyst-mediated conversion of reactants is monitored in six different solvents, all commonly used in synthetic organic chemistry. However, to be able to compare product formation in different solvents in an activity assessment, the solvent-specific APCI-MS response of the product has to be calibrated.

The relative MS responses of the product in the different solvents were determined by the triplicate injection of different concentrations (5–250 nM) of in-house-synthesised

product standard into the online system. To replicate product responses under the actual reaction detection conditions, the standards were injected into a stream of reactants (**3** and **4**). Due to the absence of catalyst, the SIM (m/z 310.2) product response directly relates to the concentration of injected product. From the integrated SIM traces, solvent-specific calibration lines were constructed with good linearity (correlation coefficients between 0.9920 (acetonitrile) and 1.0000 (methanol) with a maximum residual standard deviation (RSD) of 4.9%). The normalised slopes of the product MS response calibration lines are compared in Figure 7.

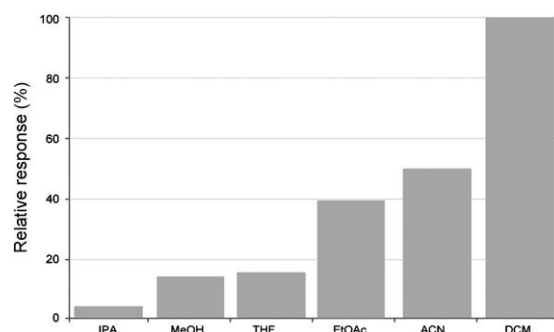


Figure 7. Relative APCI-MS response of product standard in THF, MeOH, isopropylalcohol (IPA), acetonitrile (ACN), ethylacetate (EtOAc) and dichloromethane (CH_2Cl_2).

Activity assessment of a ferrocene library: An important tool for optimising homogeneous catalysis is the application of stabilising ligands to alter the catalytically active (transition) metal centre. By applying these complexes, it is possible to optimise substrate conversion kinetics and to steer stereo-, regio- and/or enantioselectivities. This ability to affect the synthesis is based upon a combination of the electronic and steric parameters of the AgOTf–ferrocene catalyst complex involved.

Ever since the discovery of ferrocene, the special properties of this metallocene have led to an ever-increasing number of applications involving this aromatic scaffold in catalysis, in electrochemistry and in coordination chemistry. In addition to the possibility of designing specific ferrocene ligands for specific applications, a major advantage of the scaffold is its very high stability; ferrocene-based catalysts are resistant to high temperatures and humidities and can cope with a multitude of different reagents. Combined with the low prices for ferrocene, the aforementioned factors result in great application potential of ferrocene-based catalysts in industrial processes.

In the first stage of the reaction optimisation strategy, a number of metal triflates were screened for activity in the synthetic conversion that gives target molecule **5**. To broaden the range of the methodology, we screened a small ferrocene library for activity. The ferrocenes were mixed with AgOTf (1:1) prior to the activity assessment to form catalyst complexes. This ferrocene library is composed of some in-

house-produced ferrocene catalyst ligands (**6 a–h**) and several commercially available Josiphos (**7 a–d**), Taniaphos (**8 a,b**), Walphos (**9 a,b**) and a Mandyphos (**10**) ferrocene catalyst ligand(s).

The activity of the ferrocenes was determined in a high-throughput experiment and involved performance screening in six different solvents.

The results of this screening confirm the ability to screen ferrocene-ligated catalyst complexes in the selected reaction by using the MS-based continuous-flow reaction detection system. The different product yields in this activity assessment can be directly compared by correcting the results for the different catalyst concentrations and APCI-MS responses in different solvents. The results of this assay are presented in Figure 8. The steric effects introduced by the different

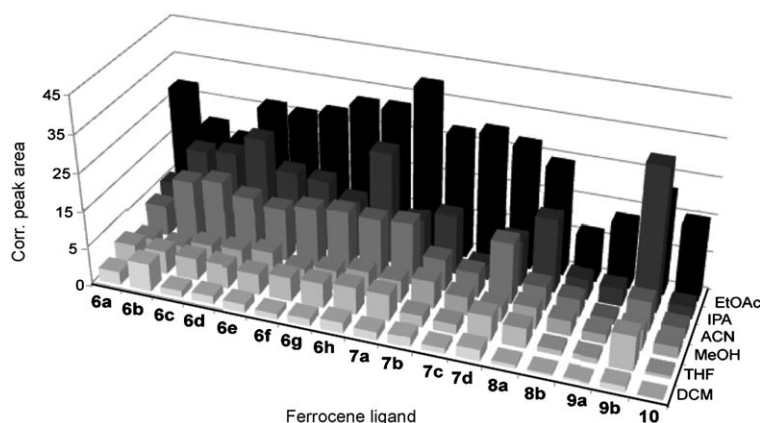


Figure 8. Activity assessment of the ferrocene library in different solvents.

catalyst complexes are of the same order of magnitude and, therefore, catalyst performance is found to be comparable. The catalyst activity in the different solvents is influenced by the solvent properties. The activity in ethylacetate was found superior and was significantly better than the performance in dichloromethane. In general, ferrocenes **10**, **8b** and **9b** were rated the poorest performing catalysts for this conversion, whereas ferrocenes **7a**, **6c** and **6h** were found to be the best performing catalysts. From these results, different activities introduced by different ferrocene types can be distinguished. Moreover, additional steric hindrance introduced by different substituents, such as in ferrocenes **9a** and **9b**, result in reduced activities. Because the HPLC pumps used in the setup were unable to cope with CH_2Cl_2 , a different setup was used for assaying the conversion in this solvent. The two reactant pumps were replaced by pumps that could pump CH_2Cl_2 and the water make-up flow was omitted because of the immiscibility. Although this setup changes the related flow rates and APCI performance, the results could still be directly compared by accurately controlling reactant flow rates and the calibration of the MS responses.

Conclusion

We have presented an alternative integrated continuous-flow reaction detection system for common homogeneous catalyst development approaches based on autonomous systems for the catalysed conversion of reactants and the determination of product formation. In the comprehensive integrated reaction detection analysis system, these segregated systems were merged into a single integrated continuous-flow system. A great virtue of the screening methodology currently described is that the versatility of traditional approaches is preserved. This is demonstrated by the employment of the same system for an automated optimisation of rudimentary reaction parameters and for the performance screening of ferrocene-based catalyst complexes. In the first

type of experiment, optimum substrate ratios, catalyst concentrations and reaction temperatures were determined unsupervised. In the second type of experiment, the applicability of the system was expanded by proof of its ability to screen for different activities related to steric parameters introduced by different ferrocene backbone substituents. Because of the HPLC equipment on which this system is based, a high degree of automation could be achieved while the reaction detection methodology circumvented the need to use sequential unit operations for the transfer of

liquids. Moreover, by integrating the workflow into a single system setup, reaction optimisation and activity assessment procedures are significantly simplified.

The pertinence of the reaction detection methodology was further improved by the considerably increased throughput accomplished by the reduction of the number of data points required for an activity assessment. For this methodology to be able to screen catalysts based on a single time-point, it must allow for sensitive quantification of the product with high accuracy at a reaction time that only slightly exceeds the time period required for the reaction to reach the initial rate. This was accomplished by the implementation of MS detection for sensitive simultaneous monitoring of the reactant- and product-related ions involved in catalyst-induced product formation. The current trend in screening assays is the downscaling of assays to reduce the amount of involved entities (catalysts and solvents) in an attempt to preserve both economical and environmental resources. The main disadvantage of miniaturising dimensions is the proportional reduction in formed product and the increased detection sensitivities required. Because of the intrinsic nature of the APCI process, APCI-MS is ideally suited to cope with these demands. We have proved this by

demonstrating the MS detection of low concentrations of converted product, thereby preserving valuable catalysts and reactants.

The main prerequisite of a detector in catalyst performance screening of synthetic conversions is its applicability in different solvents. APCI-MS can be used to determine product-related ions in a wide variety of different applications, due to the multitude of gas- and solution-phase mechanisms that convert neutral molecules into ionic species. However, concerning the applicability in different solvents, the usefulness is somewhat restricted to solvents associated with LC and GC separations. We demonstrated the feasibility of using APCI-MS for reaction detection in six different solvents that are commonly used in synthetic chemistry. To be able to compare catalyst-mediated product formation in different solvents, the system was calibrated for solvent-specific MS responses before the activity assessment was conducted. Although dichloromethane required slight system modifications due to the calibration of the MS responses, a direct comparison between the activity assays conducted in the six different solvents could still be achieved.

Experimental Section

Materials: The activity assay of the ferrocene library was conducted in six different solvents; GC-grade (>99%) THF and dichloromethane were purchased from Fluka (Buchs, Switzerland), methanol (absolute ULC/MS grade) and acetonitrile (HPLC-S grade) were purchased from Biosolve (Valkenswaard, the Netherlands). 2-propanol (>99.8%) and ethyl acetate (>99.5%) were purchased from Sigma Aldrich (Steinheim, Germany).

The applied MCR involved three different reactants; acetone (>99%) was purchased from J. T. Baker (Deventer, the Netherlands), benzylamine was purchased from Fluka (Buchs, Switzerland), and the product standards of **4** and **5** were synthesised in-house. The silver in the catalyst complexes was obtained by dissolving silver trifluoromethanesulfonate (silver triflate, AgOTf, >98%) from Fluka (Buchs, Switzerland) in the appropriate solvent. The other triflates that were used in the preliminary Lewis acid catalyst screening (Zn(OTf)₂, Yb(OTf)₃, LiOTf, Hf(OTf)₃, Sc(OTf)₃, Cu(OTf)₂ and Bi(OTf)₃) were obtained from either Sigma-Aldrich or Fluka. Water was produced in-house by using a Millipore Academic water purifier (Molsheim, France) and degassed by using a Branson ultrasonic bath (Danbury, USA). Formic acid (98%) was purchased from J. T. Baker (Deventer, the Netherlands). The ferrocene catalyst ligand library that was assayed was obtained from two different sources. The first part of the library (**6a–g**; see Figure 2), were synthesised in six steps starting from ferrocenecarboxaldehyde by using literature procedures.^[13] The second part of the ferrocene library contained ligands of the Josiphos, Walphos, Mandyphos, and Taniaphos ferrocene type, which were obtained from Sigma-Aldrich (Steinheim, Germany). The synthesis procedure and NMR spectroscopy and high-resolution MS conformation of these ferrocenes is described in the Supporting Information.

Reaction detection system: The analytical system (see Figure 1) that was used for the reaction optimisation and activity assessment of the ferrocene library involved mixing the reactants, injecting the catalysts, converting the reactants and detecting the product in a single comprehensive continuous-flow reaction detection system. The substrate delivery configuration was adapted based on the applied solvent. If THF, acetonitrile, methanol, ethyl acetate or 2-propanol were used, the mixing of reactants was performed by using two Shimadzu LC-20AD HPLC pumps (Shimadzu, 's-Hertogenbosch, the Netherlands) into a mixer (Valco International, Schenkong, Switzerland). A third LC-20AD HPLC pump was used

to increase detector compatibility by adding a water make-up flow. If dichloromethane was used the substrate delivery was performed by using two Gilson model 302 HPLC pumps (Gilson, Villiers-le-Bel, France) due to equipment incompatibilities. Due to solvent immiscibility, the water make-up flow had to be omitted in experiments conducted in dichloromethane. The injection of catalyst–ligand complexes into the stream of reactants was performed by using a fully programmable Gilson 231 auto-injector (Gilson, Villiers-le-Bel, France). The conversion into product occurred in a coiled open tubular reactor (produced in-house) immersed in a temperature-controlled water bath (Grant, Cambridge, England). The quantification of catalyst-mediated product formation was performed by using SIM in a LCMS-2010EV single-stage quadrupole mass spectrometer (Shimadzu, 's-Hertogenbosch, the Netherlands) equipped with an APCI source and operating in positive-ion mode. Measurements were performed by alternating between the SIM of the product and intermediate imine (*m/z* 310.2 and 148.1, respectively) and a full-spectrum TIC.

Acknowledgements

This work was financially supported by an ECHO grant from the Dutch Scientific Society NOW. Shimadzu Benelux is acknowledged for the loan of the LCMS-2010EV single-stage quadrupole mass spectrometer. Solvias is acknowledged for providing Josiphos, Walphos, Mandyphos and Taniaphos ferrocene catalyst ligands.

- [1] For selected reviews on combinatorial methods for the discovery of homogeneous catalysts, see: a) A. Hagemeyer, B. Jandeleit, Y. Liu, D. M. Poorjary, H. W. Turner, A. F. Volpe, Jr., W. H. Weinberg, *Appl. Catal. A* **2001**, 221, 23–43; b) B. Jandeleit, D. J. Schaefer, T. S. Powers, H. W. Turner, W. H. Weinberg, *Angew. Chem.* **1999**, 111, 2648–2689; *Angew. Chem. Int. Ed.* **1999**, 38, 2494–2532; c) W. F. Maier, K. Stöwe, S. Sieg, *Angew. Chem.* **2007**, 119, 6122–6179; *Angew. Chem. Int. Ed.* **2007**, 46, 6016–6067; d) M. T. Reetz, *Angew. Chem.* **2008**, 120, 2592–2626; *Angew. Chem. Int. Ed.* **2008**, 47, 2556–2588; e) J. M. Serra, A. Corma, S. Valero, E. Argente, V. Botti, *QSAR Comb. Sci.* **2007**, 26, 11–26.
- [2] a) R. A. Potyrailo, *TrAC, TrAC Trends Anal. Chem. Trends Anal. Chem.* **2003**, 23, 374–384; b) M. B. Onaran, C. T. Seto, *J. Org. Chem.* **2003**, 68, 8136–8141; c) M. T. Reetz, A. Zonta, K. Schimossek, K. Liebeton, K.-E. Jaeger, *Angew. Chem.* **1997**, 109, 2961–2963; *Angew. Chem. Int. Ed. Engl.* **1997**, 36, 2830–2832.
- [3] D. Fabris, *Mass Spectrom. Rev.* **2005**, 24, 30–54.
- [4] a) W. Henderson, B. K. Nickleson, L. J. McCaffrey, *Polyhedron* **1998**, 17, 4291–4313; b) J. C. Traeger, *Int. J. Mass Spectrom.* **2000**, 200, 387–401.
- [5] a) H. R. Sahoo, J. G. Kralj, K. F. Jensen, *Angew. Chem.* **2007**, 119, 5806–5810; *Angew. Chem. Int. Ed.* **2007**, 46, 5704–5708; b) D. Belder, M. Ludwig, L.-W. Wang, M. T. Reetz, *Angew. Chem.* **2006**, 118, 2523–2526; *Angew. Chem. Int. Ed.* **2006**, 45, 2463–2466; c) O. Trapp, S. K. Weber, S. Bauch, T. Bäcker, W. Hofstadt, B. Spliethoff, *Chem. Eur. J.* **2008**, 14, 4657–4666; d) O. Trapp, S. K. Weber, S. Bauch, W. Hofstadt, *Angew. Chem.* **2007**, 119, 7447–7451; *Angew. Chem. Int. Ed.* **2007**, 46, 7307–7310; e) N. Nikbin, M. Ladlow, S. V. Ley, *Org. Process Res. Dev.* **2007**, 11, 458–462; f) J. Kobayashi, Y. Mori, K. Okamoto, R. Akiyama, M. Ueno, T. Kitamori, S. Kobayashi, *Science* **2004**, 304, 1305–1308.
- [6] a) N. W. Hird, *Drug Discovery Today* **1999**, 4, 265–274; b) M. S. Congreve, C. Jamieson, *Drug Discovery Today* **2002**, 7, 139–142; c) M. D. Bowman, M. M. Jacobson, B. G. Pujanauskis, H. E. Blackwell, *Tetrahedron* **2006**, 62, 4715–4727.
- [7] C. T. Martha, N. Elders, J. G. Krabbe, J. Kool, W. M. A. Niessen, R. V. A. Orru, H. Irth, *Anal. Chem.* **2008**, 80, 7121–7127.
- [8] a) R. S. Bon, C. Hong, M. J. Bouma, R. F. Schmitz, F. J. J. de Kanter, M. Lutz, A. L. Spek, R. V. A. Orru, *Org. Lett.* **2003**, 5, 3759–3762; b) R. S. Bon, B. van Vliet, N. E. Sprengels, R. F. Schmitz, F. J. J.

- de Kanter, C. V. Stevens, M. Swart, F. M. Bickelhaupt, M. B. Groen, R. V. A. Orru, *J. Org. Chem.* **2005**, *70*, 3542–3553; c) N. Elders, R. F. Schmitz, F. J. J. de Kanter, E. Ruijter, M. B. Groen, R. V. A. Orru, *J. Org. Chem.* **2007**, *72*, 6135–6142.
- [9] For illustrative reviews concerning multicomponent reactions, see: a) R. W. Armstrong, A. P. Combs, P. A. Tempest, S. D. Brown, T. A. Keating, *Acc. Chem. Res.* **1996**, *29*, 123–131; b) L. F. Tietze, A. Modi, *Med. Res. Rev.* **2000**, *20*, 304–322; c) A. Dömling, I. Ugi, *Angew. Chem.* **2000**, *112*, 3300–3344; *Angew. Chem. Int. Ed.* **2000**, *39*, 3168–3210; d) A. Domling, *Comb. Chem. High Throughput Screening* **1998**, *1*, 1–22; e) R. V. A. Orru, M. de Greef, *Synthesis* **2003**, 1471–1499; f) J. Zhu, *Eur. J. Org. Chem.* **2003**, 1133–1144; g) H. Bienaymé, C. Hulme, G. Oddon, P. Schmitt, *Chem. Eur. J.* **2000**, *6*, 3321–3329.
- [10] a) P. Bousquet, J. Feldman, J. Schwartz, *J. Pharmacol. Exp. Ther.* **1984**, *230*, 232–236; b) A. Parini, C. Gargalidis Moudanos, N. Pizzinat, S. M. Lanier, *Notes TiPS Zeitschrift wurde bereits 1975 stillgelegt!* **1996**, *17*, 13–16; c) C. Dardonville, I. Rozas, *Med. Res. Rev.* **2004**, *24*, 639–661.
- [11] Examples of biological functions of the imidazoline binding site: hypertension: a) P. Bousquet, J. Feldman, *Drugs* **1999**, *58*, 799–812; anti-inflammation: b) M. Ueno, K. Imaizumi, T. Sugita, I. Takata, M. Takeshita, *Int. J. Immunopharmac.* **1995**, *1*, 597–603; anti-hyperglycemia: c) M. E. Doyle, J. M. Egan, *Pharmacol. Rev.* **2003**, *55*, 105–131; hormonal effects: d) M. von Rauch, M. Schlenk, R. Gust, *J. Med. Chem.* **2004**, *47*, 915–927; human brain disorders: e) A. Holt, *J. Psychiatry Neurosci.* **2003**, *28*, 409–414.
- [12] a) C. Botteghi, A. Schionato, G. Chelucci, H. Brunner, A. Kurzinger, U. Obermann, *J. Organomet. Chem.* **1989**, *370*, 17–31; b) T. Morimoto, K. Tachibana, K. Achiwa, *Synlett* **1997**, 783–785; c) A. J. Davenport, D. L. Davies, J. Fawcett, D. R. J. Russell, *J. Chem. Soc. Perkin Trans. 1* **2001**, *1*, 1500–1503; d) F. Menges, M. Neuburger, A. Pfaltz, *Org. Lett.* **2002**, *4*, 4713–4716; e) C. A. Busacca, D. Grossbach, R. C. So, E. M. O'Brien, E. M. Spinelli, *Org. Lett.* **2003**, *5*, 595–598; f) M. Casey, M. P. Smyth, *Synlett* **2003**, 102–106; g) E. Guiu, C. Claver, J. Benet-Buchholz, S. Castillon, *Tetrahedron: Asymmetry* **2004**, *15*, 3365–3373; h) A. Bastero, C. Claver, A. Ruiz, S. Castillon, E. Daura, C. Bo, E. Zangrando, *Chem. Eur. J.* **2004**, *10*, 3747–3760; i) T. Arai, T. Mizukami, N. Yokoyama, D. Nakazato, A. Yanagisawa, *Synlett* **2005**, 2670–2672; j) G. Anilkumar, S. Bhor, M. K. Tse, M. Klawonn, B. Bitterlich, M. Beller, *Tetrahedron: Asymmetry* **2005**, *16*, 3536–3561; k) M. E. Weiss, D. F. Fischer, Z.-Q. Xin, S. Jautze, W. B. Schweizer, R. Peters, *Angew. Chem.* **2006**, *118*, 5823–5827; *Angew. Chem. Int. Ed.* **2006**, *45*, 5694–5698; l) K. Ma, J. You, *Chem. Eur. J.* **2007**, *13*, 1863–1871; m) S. Jautze, P. Seiler, R. Peters, *Angew. Chem.* **2007**, *119*, 264–268; *Angew. Chem. Int. Ed.* **2007**, *46*, 1260–1264.
- [13] Synthesis of the ferrocene template **6h**: a) C. R. Hauser, J. K. Lindsay, *J. Org. Chem.*, **1957**, *22*, 906–908; b) D. Marquarding, H. Klusacek, G. Gokel, P. Hoffmann, I. Ugi, *J. Am. Chem. Soc.*, **1970**, *92*, 5389–5393; c) T. Hayashi, T. Mise, M. Fukushima, M. Kagotani, N. Nagashima, Y. Hamada, A. Matsumoto, S. Kawakami, M. Konishi, K. Yamamoto, M. Kumada, *Bull. Chem. Soc. Jpn.*, **1980**, *53*, 1138–1151. The substitution (with retention of configuration): d) T. Hayashi, A. Yamazaki, *J. Organomet. Chem.*, **1991**, *413*, 295–302; e) G. W. Gokel, D. Marquarding, I. Ugi, *J. Org. Chem.*, **1972**, *37*, 3052–3058).

Received: February 5, 2009

Published online: June 23, 2009